

Asteroid models from the Lowell Photometric Database

J. Ďurech¹, J. Hanuš^{2,3}, D. Oszkiewicz⁴, and R. Vančo⁵

¹ Astronomical Institute, Faculty of Mathematics and Physics, Charles University in Prague, V Holešovičkách 2, 180 00 Prague 8, Czech Republic

e-mail: durech@irrah.troja.mff.cuni.cz

² Centre National d'Études Spatiales, 2 place Maurice Quentin, 75039 Paris cedex 01, France

³ Laboratoire Lagrange, UMR7293, Université de la Côte d'Azur, CNRS, Observatoire de la Côte d'Azur, Blvd de l'Observatoire, CS 34229, 06304 Nice cedex 04, France

⁴ Astronomical Observatory Institute, Faculty of Physics, A. Mickiewicz University, Słoneczna 36, 60-286 Poznań, Poland

⁵ Czech National Team

Received ?; accepted ?

ABSTRACT

Context. Information about shapes and spin states of individual asteroids is important for the study of the whole asteroid population. For asteroids from the main belt, most of the shape models available now have been reconstructed from disk-integrated photometry by the lightcurve inversion method.

Aims. We want to significantly enlarge the current sample (~350) of available asteroid models.

Methods. We use the lightcurve inversion method to derive new shape models and spin states of asteroids from the sparse-in-time photometry compiled in the Lowell Photometric Database. To speed up the time-consuming process of scanning the period parameter space through the use of convex shape models, we use the distributed computing project Asteroids@home, running on the Berkeley Open Infrastructure for Network Computing (BOINC) platform. This way, the period-search interval is divided into hundreds of smaller intervals. These intervals are scanned separately by different volunteers and then joined together. We also use an alternative, faster, approach when searching the best-fit period by using a model of triaxial ellipsoid. By this, we can independently confirm periods found with convex models and also find rotation periods for some of those asteroids for which the convex-model approach gives too many solutions.

Results. From the analysis of Lowell photometric data of the first 100,000 numbered asteroids, we derived 328 new models. This almost doubles the number of available models. We tested the reliability of our results by comparing models that were derived from purely Lowell data with those based on dense lightcurves, and we found that the rate of false-positive solutions is very low. We also present updated plots of the distribution of spin obliquities and pole ecliptic longitudes that confirm previous findings about a non-uniform distribution of spin axes. However, the models reconstructed from noisy sparse data are heavily biased towards more elongated bodies with high lightcurve amplitudes.

Conclusions. The Lowell Photometric Database is a rich and reliable source of information about the spin states of asteroids. We expect hundreds of other asteroid models for asteroids with numbers larger than 100,000 to be derivable from this data set. More models will be able to be reconstructed when Lowell data are merged with other photometry.

Key words. Minor planets, asteroids: general, Methods: data analysis, Techniques: photometric

1. Introduction

Large all-sky surveys like Catalina, Pan-STARRS, etc. image the sky every night to discover new asteroids and detect those that are potentially hazardous. The main output of these surveys is a steadily increasing number of asteroids with known orbits. Apart from astrometry that is used for orbit computation, these surveys also produce photometry of asteroids. This photometry contains, in principle, information about asteroid rotation, shape, and surface properties. However, because of its poor quality (when compared with a dedicated photometric measurements of a single asteroid) the signal corresponding to asteroid's rotation is usually drowned in noise and systematic errors. However, there have been recent attempts to use sparse-in-time photometry to reconstruct the shape of asteroids. Kaasalainen (2004) has shown that sparse photometry can be used to solve the lightcurve inversion problem and further simulations confirm this (Ďurech et al. 2005; Ďurech et al. 2007). Afterwards, real sparse data were used either alone or in combination with dense

lightcurves and new asteroid models were derived (Ďurech et al. 2009; Cellino et al. 2009; Hanuš et al. 2011, 2013c). The aim of these efforts was to derive new unique models of asteroids, i.e., their sidereal rotation periods, shapes, and direction of spin axis.

Another approach to utilize sparse data was to look for changes in the mean brightness as a function of the aspect angle, which led to estimations of spin-axis longitudes for more than 350,000 asteroids (Bowell et al. 2014) from the so-called Lowell Observatory photometric database (Oszkiewicz et al. 2011).

In this paper, we show that the Lowell photometric data set can be also be used for solving the full inversion problem. By processing Lowell photometry for the first 100,000 numbered asteroids, we derived new shapes and spin states for 328 asteroids, which almost doubles the number of asteroids for which the photometry-based physical model is known.

We describe the data, the inversion method, and the reliability tests in Sect. 2, the results in Sect. 3, and we conclude in Sect. 4

2. Method

The lightcurve inversion method of Kaasalainen et al. (2001) that we applied was reviewed by Kaasalainen et al. (2002) and more recently by Ďurech et al. (2016). We used the same implementation of the method as Hanuš et al. (2011), where the reader is referred to for details. Here we describe only the general approach and the details specific for our work.

2.1. Data

As the data source, we used the Lowell Observatory photometric database (Bowell et al. 2014). This is photometry provided to Minor Planet Centre (MPC) by 11 of the largest surveys that were re-calibrated in the V-band using the accurate photometry of the Sloan Digital Sky Survey. Details about the data reduction and calibration can be found in Oszkiewicz et al. (2011). The data are available for about $\sim 330,000$ asteroids. Typically, there are several hundreds of photometric points for each asteroid. The length of the observing interval is ~ 10 – 15 years. The largest amount of data is for the low-numbered asteroids and decreases with increasing asteroid numbers. For example, the average number of data points is ~ 480 for asteroids with number $< 10,000$ and ~ 45 for those $> 300,000$. The accuracy of the data is around 0.10 – 0.20 mag.

For each asteroid and epoch of observation, we computed the asteroid-centric vectors towards the Sun and the Earth in the Cartesian ecliptic coordinate frame – these were needed to compute the illumination and viewing geometry in the inversion code.

2.2. Convex models

To derive asteroid models from the optical data, we used the lightcurve inversion method of Kaasalainen & Torppa (2001) and Kaasalainen et al. (2001), the same way as Hanuš et al. (2011). Essentially, we searched for the best-fit model by densely scanning the rotation period parameter space. We decided to search in the interval of 2–100 hours. The lower limit roughly corresponds to the observed rotation limit of asteroids larger than ~ 150 m (Pravec et al. 2002), the upper limit was set arbitrarily to cover most of the rotation periods for asteroids determined so far. For each trial period, we started with ten initial pole directions that were isotropically distributed on a sphere. This turned out to be enough not to miss any local minimum in the pole parameter space. In each period run, we recorded the period and χ^2 value that correspond to the best fit. Then we looked for the global minimum of χ^2 on the whole period interval and tested the uniqueness and stability of this globally best solution (see details in Sect. 2.6).

For a typical data set, the number of trial periods is 200,000–300,000, which takes about a month on one CPU. Because the number of asteroids we wanted to process was $\sim 100,000$, the only way to finish the computations in a reasonable time was to use tens of thousands of CPUs. For this task, we used the distributed computing project Asteroids@home.¹

2.3. Asteroids@home

Asteroids@home is a volunteer-based computing project built on the Berkeley Open Infrastructure for Network Computing (BOINC) platform. Because the scanning of the period param-

eter space is the so-called embarrassingly parallel problem, we divided the whole interval of 2–100 hours into smaller intervals (typically hundreds), which were searched individually on the computers of volunteers connected to the project. The units sent to volunteers had about the same CPU-time demand. Results from volunteers were sent back to the BOINC server and validated. When all units belonging to one particular asteroid were ready, they were connected and the global minimum was found. The technical details of the project are described in Ďurech et al. (2015)

2.4. Ellipsoids

To find the rotation period in sparse data, we also used an alternative approach that was based on the triaxial ellipsoid shape model and a geometrical light-scattering model (Kaasalainen & Ďurech 2007). Its advantage is that it is much faster than using convex shapes because the brightness can be computed analytically (it is proportional to the illuminated projected area, Ostro & Connelly 1984). On top of that, contrary to the convex modelling, all shape models automatically fulfill the physical condition of rotating along the principal axis with the largest momentum of inertia. The accuracy of this simplified model is sufficient to reveal the correct rotation period as a significant minimum of χ^2 in the period parameter space. That period is then used as a start point for the convex inversion for the final model. In many cases when the convex models gives many equally good solutions with different periods, this method provides a unique and correct rotation period.

2.5. Restricted period interval

As mentioned above, the interval for period search was 2–100 hours. However, for many asteroids, their rotation period is known from observations of their lightcurves. The largest database of asteroid rotation periods is the Lightcurve Asteroid Database (LCDB) compiled by Warner et al. (2009) and regularly updated at <http://www.minorplanet.info/lightcurvedatabase.html>. If we take information about the rotation period as an a priori constraint, we can narrow the interval of possible periods and significantly shrink the parameter space. For this purpose, we used only reliable period determinations from LCDB with quality codes U equal to 3, 3-, or 2+. However, even for these quality codes, the LCDB period can be wrong (for examples see Marciniak et al. 2015) resulting in a wrong shape model. For quality codes 3 and 3-, we restricted the search interval to $P \pm 0.05P$, where P was the rotation period reported in LCDB. Similarly for U equal to 2+, we restricted the search interval to $P \pm 0.1P$. We applied this approach to both convex- and ellipsoid-based period search.

2.6. Tests

For each periodogram, there is formally one best model that corresponds to the period with the lowest χ^2 . However, the global minimum in χ^2 has to be significantly deeper than all other local minima to be considered as a reliable solution, rather than just a random fluctuation. We could not use formal statistical tools to decide whether the lowest χ^2 value is statistically significant or not, because the data were also affected by systematic errors. Instead, to select only robust models, we set up several tests, which each model had to pass to be considered as a reliable model.

¹ <http://asteroidsathome.net>

1. The lowest χ^2 corresponding to the rotation period P_{\min} is a least 5% lower than all other χ^2 values for periods outside the $P_{\min} \pm 0.5P_{\min}^2/\Delta T$ interval, where ΔT is the time span of observations (Kaasalainen 2004). The value of 5% was chosen such that the number of unique models was as large as possible while keeping the number of a false positive solution very low ($\sim 1\%$). The comparison was done with respect to models in DAMIT (see Sect. 3.1).
2. When using convex models for scanning the period parameter space, we ran the period search for two resolutions of the convex model – the degree and order of the harmonics series expansion that parametrized the shape was three or six. The periods P_{\min} corresponding to these two resolutions had to agree within their errors (and both had to pass the test nr. 1)
3. Because we realized that $P_{\min} \gtrsim 20$ h often produced false positive solutions, we accepted only models with P_{\min} shorter than 20 hours (when there was no information about the rotation period from LCDB).
4. For a given P_{\min} , there are no more than two distinct (farther than 30° apart) pole solutions with χ^2 at least 5% deeper than other poles.
5. Because of the geometry limited close to the ecliptic plane two models that have the same pole latitudes β and pole longitudes λ that are different by 180° provide the same fit to disk-integrated data, and they cannot be distinguished from each other (Kaasalainen & Lamberg 2006). Therefore we accepted only such solutions that fulfilled the condition that if there were two pole directions (λ_1, β_1) and (λ_2, β_2) , the difference in ecliptic latitudes $|\beta_1 - \beta_2|$ has to be less than 50° and the difference in ecliptic longitudes $\text{mod}(|\lambda_1 - \lambda_2|, 180^\circ)$ has to be larger than 120° .
6. The ratio of the moment of inertia along the principal axis to that along the actual rotation axis should be less than 1.1. Otherwise the model is too elongated along the direction of the rotation axis and it is not considered a realistic shape.
7. For each asteroid that passed the above test, we created a bootstrapped lightcurve data set by randomly selecting the same number of observations from the original data set. This new data set was processed the same way as the original one (using either convex shapes or ellipsoids for the period search) and the model was considered stable only if the best-fit period P_{\min} from the bootstrapped data agreed with that from the original data.
8. We also visually checked all shape models, periodograms, and fits to the data to be sure that the shape model looked realistic and that there were no clear problems with the data and residuals. In some rare cases we rejected models that formally fitted the data, passed all the test, but were unrealistically elongated or flat.

3. Results

3.1. Comparison with independent models

From all ~ 600 models that successfully passed the tests described in Sect. 2.6, some were already modeled from other photometric data and the models were stored in the Database of Asteroid Models from Inversion Techniques (DAMIT², Ďurech et al. 2010). For this subset, we could compare our results from an inversion of Lowell data with independent models (assumed to be reliable) from DAMIT. In total, there were 279

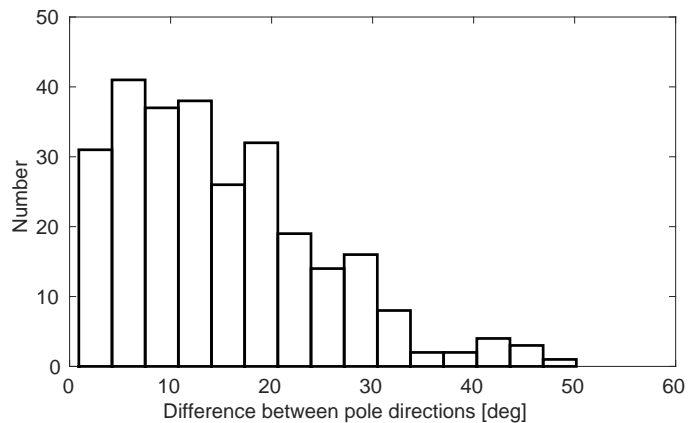


Fig. 1. Histogram of differences between the pole directions of models derived from Lowell data and those archived in DAMIT.

models in DAMIT for comparison. For these models, we computed the difference between the DAMIT and Lowell rotation periods and also the difference between the pole directions. Out of this set, almost all (275 models) have the same rotation periods (within the uncertainties) and the pole differences $< 50^\circ$ of arc. The histogram of pole differences between DAMIT and our models is shown in Fig. 1. Although there are some asteroids for which we got differences as large as $\sim 40\text{--}50^\circ$, the mean value is 15° and the median 13° , which can be interpreted as a typical error in the pole determination that was based on Lowell data, assuming that the poles from DAMIT have smaller errors (typically $5\text{--}10^\circ$).

As an example of the difference between shape models, we show results for asteroid (63) Ausonia. In Fig. 2, we compare our shape model, which we derived from Lowell sparse photometry, with that obtained by inversion of dense lightcurves (Torppa et al. 2003). In general, the shapes derived from sparse photometry are more angular than those derived from dense lightcurves and often have artificial sharp edges.

The four asteroids (5) Astraea, (367) Amicita, (540) Rosamunde, and (4954) Eric, for which we got different solutions to DAMIT, are discussed below. We also discuss the five asteroids – (1753) Mieke, (2425) Shenzen, (6166) Univsima, (11958) Galiani, and (12753) Povenmire – for which there is no model in DAMIT, but the period we derived from the Lowell data does not agree with the data in LCDB.

(5) *Astraea* From Lowell data, we got two pole directions $(\lambda, \beta) = (121^\circ, -20^\circ)$ and $(296^\circ, -15^\circ)$, the former being about 60° away from the DAMIT model of Hanuš et al. (2013b) with the pole $(126^\circ, 40^\circ)$. The DAMIT model agrees with the adaptive optics data as well as with the occultation silhouette from 2008 and it is not clear why there is so large a difference in the pole direction, while the rotation periods are the same and the number of Lowell photometric points is also large (447 points).

(367) *Amicita* The model derived from Lowell data has two pole solutions $(17^\circ, -52^\circ)$ and $(194^\circ, -45^\circ)$ and rotation period of 5.05578 h, while the DAMIT model of Hanuš et al. (2011) has prograde rotation with poles of $(21^\circ, 32^\circ)$ and $(203^\circ, 38^\circ)$, with a significantly different period of 5.05502 h. However, the DAMIT model is based on sparse data from US Naval Observatory and

² <http://astro.troja.mff.cuni.cz/projects/asteroids3D>

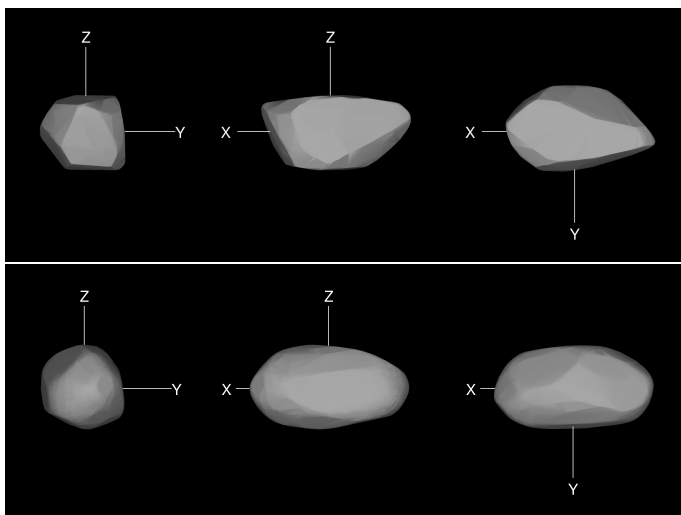


Fig. 2. Comparison between the shape model of (63) Ausonia reconstructed from Lowell sparse data (top) and from dense lightcurves (bottom).

Catalina and only two pieces of lightcurve by Wisniewski et al. (1997) and it might not be correct.

(540) Rosamunde Although the periodogram obtained with the convex model approach shows a minimum for 9.34780 h – the same as the DAMIT model of Hanuš et al. (2013a) – this minimum was not deep enough to pass the test nr. 1. However, the second-best minimum for a convex model at 7.82166 h appeared as the best solution for the ellipsoid approach and passed all tests leading to a wrong model.

(4954) Eric The DAMIT model of Hanuš et al. (2013c) has a pole direction of $(86^\circ, -55^\circ)$, which is almost exactly opposite to our value of $(261^\circ, 70^\circ)$. Moreover, even the rotation periods are different by about 0.0003 h, which is more than the uncertainty interval.

(1753) Mieke The rotation period of 8.9 h was determined by Lagerkvist (1978) from two (1.5 and 5 hours) noisy lightcurves. Given the quality of the data, this period is not in contradiction with our value of 10.19942 h.

(2425) Shenzen The rotation period of 14.715 ± 0.012 h was determined by Hawkins & Ditteon (2008). Our value of 9.83818 h is close to 2/3 of their. In the periodogram, there is no significant minimum around 14.7 h.

(6166) Univsima The lightcurve is published online in the database of R. Behrend³. However, the period of 9.6 h is based on only 12 points, which covers about half of the reported period, so we think that this preliminary result is not in contradiction with our period of ~ 11.4 h.

(11958) Galiani This asteroid was observed by Clark (2014), who determined the period 9.8013 ± 0.0023 h, which does not

agree with our value of 8.24720 h. The reason is not clear, because the data of Clark (2014) seem to fit this period correctly. We do not see any significant minimum in χ^2 near 9.8 h in the periodogram.

(12753) Povenmire The period of 12.854 h reported in the LCDB is based on the observations of Gary (2004). However, according to the same author,⁴ the correct rotation period that is based on observations from 2010 is 17.5752 ± 0.0008 h, which agrees with our value.

In summary, the frequency of false positive solutions that pass all reliability tests seems to be sufficiently low, around a few percent. However, the sample of models in DAMIT that we use for comparison is itself biased against low-amplitude long-period asteroids (Marciniak et al. 2015), so the real number of false positive solutions might be higher.

3.2. New models

After applying all the tests described in Sect. 2.6, we selected only those asteroids with no model in DAMIT for publication. These are listed in Tables 1 (models from full interval 2–100 hours) and 2 (models derived from a restricted period interval). The tables list the pole direction(s) (one or two models), the sidereal rotation period (with uncertainty corresponding to the order of the last decimal place). The C/E code means the method by which P_{\min} was found – convex models (C) or ellipsoids (E). In some cases, both methods independently gave the same value of P_{\min} (then CE code). All new shape models and the photometric data are available in DAMIT.

For some of these asteroids, Hanuš et al. (2016) obtained independent models by applying the same lightcurve inversion method on sparse data, which they combined with dense lightcurves. These asteroids (not yet published in DAMIT) are marked by asterisk in the Tables 1 and 2. For all of them (56 in total), our rotation periods agree with those of Hanuš et al. (2016) within their uncertainties and pole directions differ by 10–20 degrees on average. By way of comparison, this is a similar result to the DAMIT models (Sect. 3.1, Fig. 1) and it independently confirms the reliability of our models based on only Lowell data.

3.3. Statistics of pole directions

Together with models from DAMIT, we now have a sample of shape models for 717 asteroids (685 MBAs, 13 NEAs, 10 Mars-crossers, 7 Hungarias, 1 Hilda, and 1 Trojan). The statistical analysis of the pole distribution confirms the previous findings. Namely, the distribution of spin directions is not isotropic (Kryszczyńska et al. 2007). Moreover, the distribution of pole obliquities (an angle between the spin vector and the orbital plane) depends on the size of an asteroid. We plot the dependence of obliquity on the size in Fig. 3 for main-belt (MBAs) and near-Earth (NEAs) asteroids. There is a clear trend of smaller asteroids clustering towards extreme values of obliquity. This was explained by Hanuš et al. (2011) as YORP-induced evolution of spins (Hanus et al. 2013c). The distribution of obliquities is not symmetric around 90° (Fig. 4). As noticed by Hanuš et al. (2013c), the retrograde rotators are more concentrated to -90° , probably because prograde rotators are affected by resonances. For larger asteroids, there is an excess of pro-

³ <http://obswww.unige.ch/~behrend/page5cou.html>

⁴ <http://brucegary.net/POVENMIRE/>

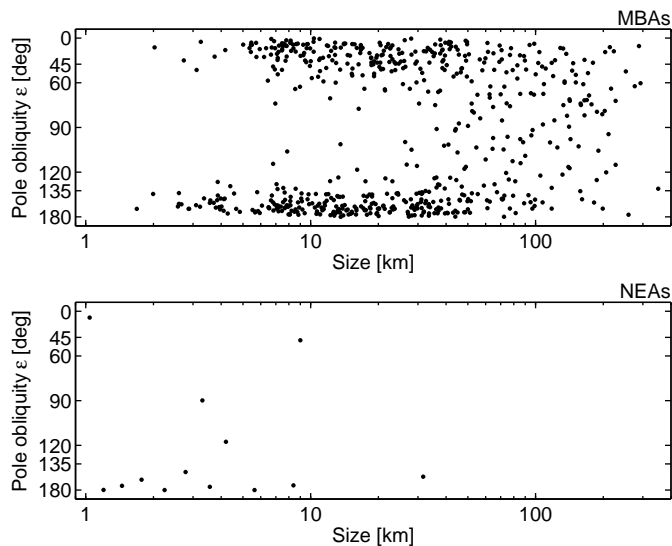


Fig. 3. The distribution of pole obliquity ε as a function of size for 575 main-belt and 13 near-Earth asteroids.

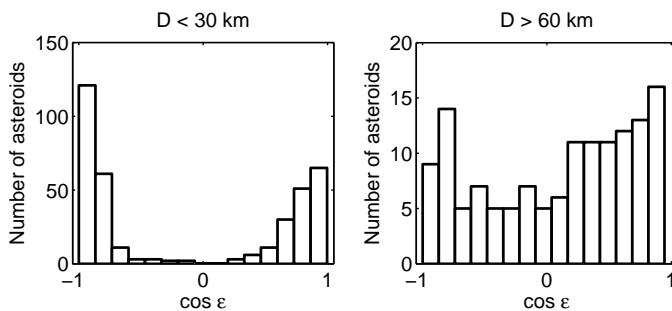


Fig. 4. Histograms of the distribution of pole obliquities ε for asteroids with diameters < 30 km and > 60 km, respectively.

grade rotators that might be primordial (Kryszczyńska et al. 2007; Johansen & Lacerda 2010).

However, the current sample of asteroid models is far from being representative of the whole asteroid population. Because the period search in sparse data is strongly dependent on the lightcurve amplitude – the larger the amplitude the easier is to detect the correct rotation period in noisy data – more elongated asteroids are reconstructed more easily than spherical ones. That is why almost all the asteroids listed in Tables 1 and 2 have large amplitudes of ≥ 0.3 mag. The lightcurve inversion (based mostly or exclusively on sparse data) is also less efficient for asteroids with poles close to the ecliptic plane because, during some apparitions, we observe them almost pole-on, thus with very small amplitudes. This bias in the method was estimated to be of the order of several tens percent (Hanuš et al. 2011). A much higher discrepancy (factor 3–4) in the successfully recovered pole directions between poles close-to and perpendicular-to the ecliptic was found by Santana-Ros et al. (2015). But even such a large selection effect cannot fully explain the significant “gap” for obliquities between 60–120°. To clearly show how the unbiased distribution of pole obliquities looks like, we would have to carry out an extensive simulation on a synthetic population with realistic systematic and random errors to see the bias that is induced by the method, shape, and geometry. This sort of simulation would be more computationally demanding than

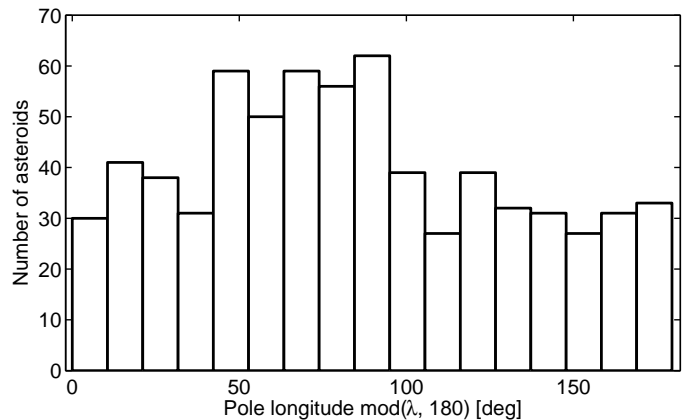


Fig. 5. Histograms of the distribution of pole longitude λ for 685 main-belt asteroids.

processing real data from the Lowell database. Therefore, we postpone this investigation for a future paper.

For near-Earth asteroids, the excess of retrograde rotators can be explained by the Yarkovsky-induced delivery mechanism from the main belt through resonances (La Spina et al. 2004), although the number of NEA models in our sample is too small for any reliable statistics.

We also see a clear deviation from a uniform distribution of pole longitudes in Fig. 5. Because of ambiguity in pole direction (often there are two solutions with similar latitudes and the difference in longitudes of about 180°), we plotted the distribution modulo 180°. The histogram shows an excess of longitudes around 50–100°. This was already announced by Bowell et al. (2014), who processed the Lowell data set using a different approach, estimated spin-axis longitudes for more than 350,000 asteroids, and revealed an excess of longitudes at 30–110° and a paucity at 120–180°. The explanation of this phenomenon remains unclear.

4. Conclusions

The new models presented in this paper significantly enlarge the sample of asteroids for which their spin axis direction and approximate shape are known. Because these models are based on a limited number of data points, the shapes have to be interpreted as only approximations of the real shapes of asteroids. Also the pole directions need to be refined with more data if one is interested in a particular asteroid. However, as an ensemble, the models can be used in future statistical studies of asteroid spins, for example.

We believe that this is only the beginning of a mass production of shape and spin models from sparse photometry. Although the number of models derivable from the Lowell Observatory photometric database is small compared to the total number of asteroids, the potential of Lowell photometry consists in its combination with other data. Even a priori information about the rotation period shrinks the parameter space that has to be scanned, and a local minimum in a large parameters space becomes a global minimum on a restricted interval. Of course, the reliability of this type of model depends critically on the reliability of the period. Lowell photometry can be combined with dense lightcurves that constrain the rotation period. This way, models for about 250 asteroids were derived recently by Hanuš et al. (2016), some of which confirm the models pre-

sented in this paper. The database of asteroid rotation periods has been increased dramatically by Waszczak et al. (2015) – their data can also be combined with Lowell photometry, and we expect that other hundreds of models will be reconstructed from this data set. Another promising approach is the combination of sparse photometry with data from the Wide-field Infrared Survey Explorer (WISE) mission (Wright et al. 2010). Although WISE data were observed in mid-infrared wavelengths, Ďurech et al. (2016) showed that thermally emitted flux can be treated as reflected light to derive the correct rotation period and the shape and spin model. This opens up a new possibility, because both Lowell and WISE data are available for tens of thousands of asteroids.

In general, the combination of more data sources is always better than using them separately. By using Lowell photometry with dense lightcurves, WISE data, photometry from Gaia, etc., the number of available models will increase and the statistical studies of spin and shape distribution will become more robust, being based on larger sets of models. Nevertheless, any inference based on the models derived from lightcurves (and sparse lightcurves in particular) has to take into account that the sample of models is biased against more spherical shapes with low lightcurve amplitudes and poles near the plane of ecliptic.

Acknowledgements. We would not be able to process data for hundreds of thousands of asteroids without the help of tens of thousand of volunteers who joined the Asteroids@home BOINC project and provided computing resources from their computers. We greatly appreciate their contribution. The work of JĎ was supported by the grant 15-04816S of the Czech Science Foundation. JH greatly appreciates the CNES post-doctoral fellowship program. JH was supported by the project under the contract 11-B556-008 (SHOCKS) of the French Agence Nationale de la Recherche (ANR). DO was supported by the grant NCN 2012/S/ST9/00022 Polish National Science Center. We thank the referee A. Marciniak for providing constructive comments that improved the contents of this paper.

References

- Bowell, E., Oszkiewicz, D. A., Wasserman, L. H., et al. 2014, *Meteoritics and Planetary Science*, 49, 95
- Cellino, A., Hestroffer, D., Tanga, P., Mottola, S., & Dell’Oro, A. 2009, *A&A*, 506, 935
- Clark, M. 2014, *Minor Planet Bulletin*, 41, 178
- Ďurech, J., Grav, T., Jedicke, R., Kaasalainen, M., & Denneau, L. 2005, *Earth, Moon, and Planets*, 97, 179
- Ďurech, J., Scheirich, P., Kaasalainen, M., et al. 2007, in *Near Earth Objects, our Celestial Neighbors: Opportunity and Risk*, ed. A. Milani, G. B. Valsecchi, & D. Vokrouhlický (Cambridge: Cambridge University Press), 191
- Ďurech, J., Kaasalainen, M., Warner, B. D., et al. 2009, *A&A*, 493, 291
- Ďurech, J., Sidorin, V., & Kaasalainen, M. 2010, *A&A*, 513, A46
- Ďurech, J., Carry, B., Delbo, M., Kaasalainen, M., & Viikinkoski, M. 2016, in *Asteroids IV*, in press, ed. P. Michel, F. DeMeo, & W. Bottke (Tucson: University of Arizona Press)
- Ďurech, J., Hanuš, J., & Vančo, R. 2015, *Astronomy and Computing*, 13, 80
- Ďurech, J., Hanuš, J., Ali-Lagoa, V., Delbo, M., & Oszkiewicz, D. 2016, in *Proceedings IAU Symposium No. 318*, in press, ed. S. Chesley, R. Jedicke, A. Morbidelli, & D. Farnocchia (Cambridge: Cambridge University Press)
- Gary, B. L. 2004, *Minor Planet Bulletin*, 31, 56
- Hanuš, J., Brož, M., Ďurech, J., et al. 2013a, *A&A*, 559, A134
- Hanuš, J., Marchis, F., & Ďurech, J. 2013b, *Icarus*, 226, 1045
- Hanuš, J., Ďurech, J., Brož, M., et al. 2013c, *A&A*, 551, A67
- Hanuš, J., Ďurech, J., Brož, M., et al. 2011, *A&A*, 530, A134
- Hanuš, J., Ďurech, J., Oszkiewicz, D. A., et al. 2016, *A&A*, in press
- Hawkins, S. & Ditteon, R. 2008, *Minor Planet Bulletin*, 35, 1
- Johansen, A. & Lacerda, P. 2010, *MNRAS*, 404, 475
- Kaasalainen, M. 2004, *A&A*, 422, L39
- Kaasalainen, M. & Ďurech, J. 2007, in *Near Earth Objects, our Celestial Neighbors: Opportunity and Risk*, ed. A. Milani, G. B. Valsecchi, & D. Vokrouhlický (Cambridge: Cambridge University Press), 151
- Kaasalainen, M. & Lamberg, L. 2006, *Inverse Problems*, 22, 749
- Kaasalainen, M., Mottola, S., & Fulchignoni, M. 2002, in *Asteroids III*, ed. W. F. Bottke, A. Cellino, P. Paolicchi, & R. P. Binzel (Tucson: University of Arizona Press), 139–150
- Kaasalainen, M. & Torppa, J. 2001, *Icarus*, 153, 24
- Kaasalainen, M., Torppa, J., & Muinonen, K. 2001, *Icarus*, 153, 37
- Kryszczyńska, A., La Spina, A., Paolicchi, P., et al. 2007, *Icarus*, 192, 223
- La Spina, A., Paolicchi, P., Kryszczyńska, A., & Pravec, P. 2004, *Nature*, 428, 400
- Lagerkvist, C.-I. 1978, *A&AS*, 31, 361
- Marciniak, A., Pilcher, F., Oszkiewicz, D., et al. 2015, *Planet. Space Sci.*, 118, 256
- Ostro, S. J. & Connelly, R. 1984, *Icarus*, 57, 443
- Oszkiewicz, D., Muinonen, K., Bowell, E., et al. 2011, *Journal of Quantitative Spectroscopy and Radiative Transfer*, 112, 1919, *electromagnetic and Light Scattering by Nonspherical Particles {XII}*
- Pravec, P., Harris, A. W., & Michałowski, T. 2002, in *Asteroids III*, ed. W. F. Bottke, A. Cellino, P. Paolicchi, & R. P. Binzel (Tucson: University of Arizona Press), 113–122
- Santana-Ros, T., Bartzczak, P., Michałowski, T., Tanga, P., & Cellino, A. 2015, *MNRAS*, 450, 333
- Torppa, J., Kaasalainen, M., Michałowski, T., et al. 2003, *Icarus*, 164, 346
- Warner, B. D., Harris, A. W., & Pravec, P. 2009, *Icarus*, 202, 134
- Waszczak, A., Chang, C.-K., Ofek, E. O., et al. 2015, *AJ*, 150, 75
- Wisniewski, W. Z., Michałowski, T. M., Harris, A. W., & McMillan, R. S. 1997, *Icarus*, 126, 395
- Wright, E. L., Eisenhardt, P. R. M., Mainzer, A. K., et al. 2010, *AJ*, 140, 1868

Table 1. List of new asteroid models derived from the full period interval 2–100 hours. For each asteroid, there is one or two pole directions in the ecliptic coordinates (λ, β), the sidereal rotation period P , rotation period from LCDB P_{LCDB} and its quality code U (if available), the minimum and maximum lightcurve amplitude A_{min} , A_{max} , respectively, the number of data points N , and the method which was used to derive the unique rotation period: C – convex inversion, E – ellipsoids, CE – both methods gave the same unique period. The accuracy of the sidereal rotation period is of the order of the last decimal place given. Asteroids marked with * were independently confirmed by Hanuš et al. (2016).

number	Asteroid name/designation	λ_1 [deg]	β_1 [deg]	λ_2 [deg]	β_2 [deg]	P [h]	P_{LCDB} [h]	A_{min} [mag]	A_{max} [mag]	U	N	method
136	Austria*	118	57	333	75	11.49665	11.4969		0.37	3	401	CE
163	Erigone	276	-69			16.1402	16.136	0.32	0.37	3	483	E
186	Celuta	88	-54	235	-77	19.8435	19.842	0.4	0.55	3	406	C
254	Augusta*	56	-69	218	-75	5.89503	5.8961	0.56	0.75	3-	371	CE
263	Dresda*	101	55	280	58	16.8138	16.809	0.32	0.55	3	605	E
274	Philagoria*	138	-52	303	-58	17.94072	17.96	0.43	0.51	3	460	E
296	Phaetusa*	145	53	326	60	4.538091	4.5385	0.38	0.50	3	340	C
381	Myrrha*	3	48	160	77	6.57198	6.572	0.35	0.36	3	496	E
407	Arachne*	64	-49	268	-63	22.6264	22.62	0.31	0.45	2	433	C
427	Galene	72	-57	272	-75	3.706036	3.705	0.55	0.68	3	394	CE
474	Prudentia*	150	-58	297	-46	8.57228	8.572	0.53	0.90	3	374	E
482	Petrina*	94	2	274	37	11.79212	11.7922	0.07	0.56	3	337	E
518	Halawe	120	-66	292	-58	14.31765	14.310	0.50	0.55	3	439	E
520	Franziska*	122	-50	301	-59	16.5044	16.507	0.35	0.51	3	384	CE
523	Ada	152	-70	357	-70	10.03242	10.03	0.52	0.70	3	343	CE
616	Elly	60	62	250	44	5.29770	5.297	0.34	0.44	3	368	CE
620	Drakonia	138	56	316	47	5.48711	5.487	0.52	0.65	3	345	E
632	Pyrrha*	72	-64	249	-72	4.116854	4.1167		0.40	3	487	CE
650	Amalasantha	46	51			16.57586	16.582	0.45	0.49	3	435	E
686	Gersuind*	127	56			6.31240	6.3127	0.30	0.37	3	400	E
689	Zita	8	-72	256	-61	6.42391	6.425	0.30	0.62	3	369	E
698	Ernestina*	193	-68			5.03661	5.0363	0.30	0.69	3	459	C
718	Erida	78	-56	257	-52	17.4462	17.447	0.31	0.37	3	430	E
749	Malzovia*	53	37	242	46	5.92749	5.9279		0.30	3-	423	E
784	Pickeringia*	99	67	283	30	13.16995	13.17	0.20	0.40	2	437	E
789	Lena	192	39			5.84239	5.848	0.40	0.50	3	328	E
829	Academia	71	-41	245	-67	7.89321	7.891	0.36	0.44	3-	436	E
877	Walkure*	68	58	253	61	17.4217	17.424	0.33	0.44	3-	596	E
881	Athene*	123	-58	337	-47	13.89449	13.895	0.39	0.53	3-	376	CE
955	Alstede	54	38	240	13	5.18735	5.19	0.26	0.27	3	401	E
996	Hilaritas	100	-56	281	-57	10.05154	10.05	0.63	0.70	3	442	CE
998	Bodea	7	-59			8.57412	8.574		0.68	3	262	E
1017	Jacqueline	7	55	170	65	7.87149	7.87	0.6	0.72	3	491	CE
1035	Amata	31	69	247	29	9.08215	9.081	0.41	0.44	3	305	E
1050	Meta	60	-42	198	-79	6.14188	6.142		0.46	3	325	E
1061	Paeonia	155	-50			7.99710	6.		0.5	2-	314	E
1075	Helina	123	-33	284	-34	44.6768	44.9		0.64	3-	421	C
1081	Reseda	92	-69	256	-76	7.30136	7.3002		0.34	3	410	E
1082	Pirola	123	-42	300	-38	15.8540	15.8525	0.53	0.60	3	528	E
1098	Hakone	40	43			7.14117	7.142	0.35	0.40	3	382	E
1119	Euboea*	71	61	280	54	11.39823	11.41	0.46	0.50	3	461	E
1121	Natascha	16	59	209	50	13.19717	13.197		0.51	3	415	E
1127	Mimi	224	-57			12.74557	12.749	0.72	0.95	3	357	CE
1135	Colchis*	7	-54	168	-56	23.4827	23.47		0.45	2	409	C
1147	Stavropolis	78	-50	267	-51	5.66079	5.66		0.42	3	372	E
1187	Afra	40	34	226	13	14.06993	14.0701	0.38	0.40	3	374	E
1204	Renzia*	130	-44	312	-51	7.88697	7.885		0.42	3	528	E
1206	Numerowia	64	-50	271	-69	4.77529	4.7743		0.63	3	322	CE
1219	Britta	72	-66	241	-66	5.57556	5.575	0.48	0.75	3	387	E
1230	Riceia	37	-63			6.67317					293	CE
1231	Auricula	57	-57	225	-85	3.981580	3.9816		0.75	3	292	E
1245	Calvinia	52	-51	235	-43	4.85148	4.84	0.37	0.7	3	410	E
1248	Jugurtha	254	-89			12.19047	12.910	0.70	1.4	3	381	C
1251	Hedera	124	-70	266	-62	19.9020	19.9000	0.41	0.61	3-	415	E
1275	Cimbria	85	-61	271	-31	5.65454	5.65	0.40	0.57	3	352	E
1281	Jeanne	153	19	338	32	15.30379	15.2		0.45	2	470	E

Table 1. continued.

number	Asteroid name/designation	λ_1 [deg]	β_1 [deg]	λ_2 [deg]	β_2 [deg]	P [h]	P_{LCDB} [h]	A_{min} [mag]	A_{max} [mag]	U	N	method
1299	Mertona	73	35	253	56	4.97691	4.977	0.46	0.59	3	369	E
1312	Vassar*	104	-50	250	-29	7.93189	7.932		0.35	3	317	E
1320	Impala	151	-57	254	-70	6.17081	6.167	0.40	0.52	2+	353	E
1334	Lundmarka	79	-75			6.25033	6.250		0.70	3-	496	CE
1339	Desagneauxa	63	53	225	42	9.37514	9.380	0.45	0.48	3	465	E
1349	Bechuana	153	32	314	46	15.6873	15.692		0.30	3-	412	E
1350	Rosselia	67	-64	246	-58	8.14008	8.140	0.3	0.54	3	425	E
1391	Carelia	21	-79	208	-43	5.87822					295	E
1400	Tirela	58	-80	297	-41	13.35384	13.356		0.55	2	281	E
1459	Magnya*	73	-54	198	-55	4.679102	4.678	0.57	0.85	3	363	E
1484	Postrema	19	44	250	64	12.18978	12.1923	0.22	0.23	3-	312	E
1493	Sigrid	183	69	350	69	43.1795	43.296	0.38	0.6	2	452	C
1494	Savo	50	-65	233	-68	5.35059	5.35011	0.45	0.52	3	486	C
1500	Jyvaskyla	123	-75	268	-79	8.82750					248	C
1545	Thernoë	164	-75	352	-80	17.20321	17.20		0.76	3	281	E
1547	Nele	159	28	318	50	7.09742	7.100	0.18	0.45	3-	343	E
1548	Palomaa	72	-61	232	-32	7.49966	7.4961		0.50	3	353	E
1551	Argelander	3	-81	183	-72	4.058350					453	CE
1557	Roehla	124	-38	329	-57	5.67899					334	CE
1561	Fricke	320	71			15.15330					395	E
1597	Laugier	345	-78			8.02272					321	E
1619	Ueta	99	49	295	37	2.718238	2.720	0.32	0.44	3	350	E
1623	Vivian	52	-66	229	-56	20.5235	20.5209		0.85	3-	316	C
1643	Brown	140	64	353	84	5.93124	5.932		0.48	3	497	CE
1648	Shajna*	94	47	278	50	6.41368	6.4140		0.65	3	391	E
1672	Gezelle*	44	73	234	82	40.6821	40.72	0.2	0.56	3	366	C
1676	Kariba*	71	74	279	56	3.167336	3.1673	0.51	0.65	3	342	CE
1687	Glarona	132	76	274	70	6.49595	6.3		0.75	3	375	CE
1730	Marceline*	95	56	303	81	3.836550	3.837	0.94	1.00	3	268	E
1733	Silke	141	-63	302	-58	7.89457					277	E
1738	Oosterhoff	121	-62	301	-80	4.448955	4.4486	0.48	0.54	3	371	C
1743	Schmidt	69	-62	261	-53	17.4599	17.45		0.36	3	381	E
1753	Mieke	121	67	321	35	10.19942	8.8		0.2	2	413	E
1758	Naantali	150	-60			5.47369	5.4699		0.44	3	446	E
1768	Appenzella	39	45	227	40	5.18335	5.1839		0.53	3	395	CE
1774	Kulikov	54	-50	237	-46	3.830791					518	E
1792	Reni	122	-41	260	-50	15.94121	15.95		0.54	3-	319	E
1793	Zoya*	52	59	227	59	5.75187	5.753		0.40	2+	398	CE
1801	Titicaca	48	51	260	57	3.211233	3.2106		0.50	3	379	CE
1814	Bach	126	66	317	64	7.23954					221	CE
1819	Laputa	149	-48			9.79965	9.8004		0.51	3	394	CE
1825	Klare*	115	-61	315	-69	4.742885	4.744	0.70	0.90	3	336	CE
1838	Ursa*	51	66	286	32	16.16358	16.141		0.80	3	346	C
1840	Hus	298	-77			4.749057	4.780		0.85	2-	549	E
1841	Masaryk	122	62	305	59	7.54301	7.53		0.52	2+	406	E
1855	Korolev	90	52	262	64	4.656199	4.6568	0.75	0.76	3	370	C
1900	Katyusha	94	-46	291	-48	9.50358	9.4999	0.56	0.74	3	283	E
1942	Jablunka	156	-73			8.91158					225	E
1945	Wesselink	190	-78	336	-60	3.547454					445	E
1949	Messina	138	-64	326	-51	3.649308	3.6491		0.37	3	323	CE
1978	Patrice	21	13	203	18	5.881213					365	CE
1985	Hopmann	107	-81			17.4787	17.480	0.36	0.44	3	272	E
1997	Leverrier	96	46	274	40	8.01532					301	E
2313	Aruna*	94	-80	283	-70	8.88618	8.90		0.79	3	715	E
2381	Landi*	54	-87	237	-45	3.986045	3.989	0.75	1.04	3	364	E
2395	Aho	160	47	340	46	7.88033					751	E
2425	Shenzhen	50	58	265	40	9.83818	14.715		0.80	3	551	E
2483	Guinevere	19	70	194	59	14.73081	14.733	1.34	1.38	3	317	E
2528	Mohler	56	-64	246	-54	6.49130					641	E
2581	Radegast	57	56	230	53	8.75121					573	CE

Table 1. continued.

number	Asteroid name/designation	λ_1 [deg]	β_1 [deg]	λ_2 [deg]	β_2 [deg]	P [h]	P_{LCDB} [h]	A_{min} [mag]	A_{max} [mag]	U	N	method
2630	Hermod	74	50	256	45	19.4283					578	E
2659	Millis*	117	-55	294	-52	6.12464	6.132	0.53	0.84	3	566	C
2836	Sobolev	82	-51	270	-79	4.754883					560	E
3086	Kalbaugh	63	-51			5.17907	5.180	0.47	0.76	3	383	C
3261	Tvardovskij	90	65	280	68	5.36852					665	E
3281	Maupertuis	62	-66	231	-74	6.72984	6.7295		1.22	3	453	E
3286	Anatoliya	52	51	293	76	5.81029					410	CE
3375	Amy	168	-50	343	-49	3.255633					486	E
3407	Jimmysimms	34	53	259	82	6.82069	6.819	0.93	0.95	3	457	E
3544	Borodino*	104	-57	267	-53	5.43459	5.442	0.60	0.65	3	515	E
3573	Holmberg	142	50	318	52	6.54245	6.5431	0.91	1.03	3	577	C
3735	Trebon	51	-54	236	-69	8.47251					568	E
3746	Heyuan	170	66	333	70	16.3010					538	E
3758	Karttunen	74	-72	202	-52	12.50101					396	CE
3786	Yamada*	100	54	205	60	4.032946	4.034	0.40	0.65	3	463	E
3822	Segovia	43	58	265	72	11.03204					585	E
3910	Liszt	104	-46	290	-66	4.736280	4.73		0.60	3	423	E
4037	Ikeya	92	67	270	44	4.057537					485	E
4877	Humboldt	218	-77	340	-55	3.491213					450	E
5006	Teller	84	66	301	57	10.90225	10.898		0.69	3	474	E
5195	Kaendler	67	-59	212	-50	5.33756					537	E
5299	Bittesini	76	60	251	49	4.679660					599	CE
5488	Kiyosato	19	23	242	62	8.76307					449	E
5489	Oberkochen*	23	-62	194	-38	5.62439	5.625	0.40	0.51	3	470	E
5494	1933 UM1	137	-65	323	-62	5.72752					612	CE
5685	Sanenobufukui	122	-63	327	-58	3.387871					518	CE
5723	Hudson	72	-73	255	-58	4.475115					472	E
5776	1989 UT2*	105	-76	350	-46	4.340787					473	E
5929	1974 XT	130	-71	244	-40	3.759432	3.7596		1.01	3	358	E
5993	Tammydickinson	52	-65	241	-78	9.44711					546	E
6136	Gryphon	134	57	337	63	16.4683	16.476		0.61	3	602	E
6161	Vojno-Yasenetsky	64	70	217	41	7.98095					393	E
6166	Univsima	80	-42	242	-59	11.37655	9.6		0.6	2	425	E
6276	Kurohone	147	63	322	62	6.34850					441	E
6410	Fujiwara*	148	-59	296	-81	7.00667	7.0073	0.80	0.85	3	552	E
6422	Akagi	213	-38			7.74756					430	E
6590	Barolo	171	59	313	63	8.35928					460	CE
6671	1994 NC1	69	57	204	78	5.22042					463	E
6719	Gallaj	60	-63	252	-59	4.429487					515	E
6882	Sormano	43	-33	248	-58	3.998344					396	E
7001	Noether	13	-66			9.58191					421	E
7072	Beijingdaxue	72	56	262	64	5.304419					549	E
7106	Kondakov	63	58	268	81	7.59690					515	E
7289	Kamegamori	108	-39	268	-54	3.831182					538	C
7318	Dyukov	65	-64	239	-44	4.856335					497	E
7835	1993 MC	72	-64	288	-55	7.43019					473	E
7896	Svejk	86	36	266	35	16.20582					500	E
7964	1995 DD2	74	-73	264	-49	10.22553					532	E
8573	Ivanka	100	-70	344	-78	8.03312					454	E
9440	1997 FZ1	97	-64	278	-65	5.196349					485	E
9971	Ishihara	42	76	223	60	6.71574					559	E
10281	1981 EE45	183	-88			7.57192					462	E
10472	1981 EO20	73	37	249	43	5.98599					344	C
10627	Ookuninushi	3	49	204	89	4.334986					394	E
11052	1990 WM	194	-49	351	-78	5.06904					471	E
11148	Einhardress	121	-69	296	-64	7.77240					378	E
11700	1998 FT115	82	-64	280	-72	5.52303					596	E
11958	Galiani	12	47			8.24720	9.801		0.96	2+	541	E
11995	1995 YB1	70	-80	238	-68	12.66498					398	E
12384	Luigimartella	4	-50	160	-60	6.44220					517	E

Table 1. continued.

number	Asteroid name/designation	λ_1 [deg]	β_1 [deg]	λ_2 [deg]	β_2 [deg]	P [h]	P_{LCDB} [h]	A_{min} [mag]	A_{max} [mag]	U	N	method
12551	1998 QQ39	123	50	299	44	11.19841					571	E
12753	Povenmire	138	-28	295	-48	17.5740	12.854		0.45	2	424	E
12774	Pfund	121	53	308	62	7.34295					174	E
12979	1978 SB8	45	-68	203	-62	5.78331					349	C
13059	Ducuroir	117	71	311	73	13.84864					560	E
13338	1998 SK119	86	-42	240	-70	4.129105					474	E
13535	1991 RS13	127	-64	318	-60	5.22705					390	E
13952	1990 SN6	13	58	193	67	7.35225					526	E
14031	1994 WF2	41	-62	180	-60	2.900652					509	E
14044	1995 VS1	95	-47	253	-57	9.25874					499	E
14203	Hocking	106	81	240	52	9.08566					393	E
14691	2000 AK119	38	-54	248	-68	3.652412	3.652	0.70	0.78	3	441	E
15677	1980 TZ5	75	-64	226	-75	5.61479					491	E
16216	2000 DR4	130	-66			10.36816					480	E
16786	1997 AT1	178	56	307	60	4.020902					296	E
16955	1998 KU48	122	-48	264	-51	5.26062					387	E
17111	1999 JH52	157	46	328	62	8.89847					629	E
19608	1999 NC57	69	-68	306	-68	9.18995					513	E
20329	Manfro	92	-55	258	-63	8.80724					395	E
20570	Molchan	40	-52	244	-59	4.132007					485	E
20725	1999 XP120	170	67	334	45	3.601296					488	E
21411	Abifraeman	249	-63			11.02020					409	E
22018	1999 XK105	61	45	228	31	17.0575					373	C
22298	1990 EJ	64	-42	244	-72	2.985538					530	C
23578	Baedeker	141	-53			8.17154					382	C
23707	1997 TZ7	185	79	334	35	5.06632					381	E
23873	1998 RL76	56	-74			13.86111					323	E
26241	1998 QY40	40	45			12.83303					380	C
26387	1999 TG2	94	-46	325	-79	5.14720					460	E
26460	2000 AZ120	9	-87	230	-47	5.45444	5.48		0.90	2	326	E
27225	1999 GB17	72	54	266	31	3.853858					480	C
28133	1998 SS130	126	-49	310	-56	5.46284					408	CE
29308	1993 UF1	71	-56	246	-83	9.79348	9.810	0.83	0.94	3	365	E
29777	1999 CK46	32	56	224	40	3.627265					460	E
31060	1996 TB6*	103	-52	253	-76	5.104323	5.103		0.80	3	394	E
32575	2001 QY78	60	-70	223	-64	4.535495	4.5344		0.86	3	324	E
32799	1990 QN1	71	75	258	72	9.49636					337	E
33776	1999 RB158	46	64	247	42	16.9593					426	E
33854	2000 HH53	114	-56	236	-78	4.423484					348	E
33974	2000 ND17	132	-55	347	-65	4.67868					340	E
34318	2000 QV192	81	-70	237	-36	6.35105					198	E
35218	1994 WU2	138	-56	304	-68	11.56991					353	E
35928	1999 JV107	137	-52	302	-75	7.26361					279	E
35965	1999 LH13	63	-70	245	-55	6.76072					387	E
36303	2000 JM54	55	-48	225	-46	4.93652					368	E
36487	2000 QJ42	127	-66	332	-50	8.14982					333	E
36944	2000 SD249	96	-69	295	-76	6.09677					188	C
40104	1998 QE4	144	-87			4.475241					443	E
40478	1999 RT54	184	-66	358	-65	3.886734					286	C
40806	1999 TX41	82	-69	269	-64	6.41500					198	C
43163	1999 XB127	154	-59			5.20660					298	C
43574	2001 FU192	104	-36	279	-49	4.324751					239	E
45864	2000 UO97	44	-66	179	-84	5.13544					436	E
46376	2001 XD3	121	55			5.73569					278	E
47508	2000 AQ58	12	-49	196	-26	5.05521					349	E
48268	2002 AK1	72	-69	234	-35	4.250546					406	E
48842	1998 BA44	86	83	254	43	6.17996					383	E
52723	1998 GP2	86	-39	224	-56	11.90781					329	E
54850	2001 OZ11	20	-68	189	-48	4.222157					283	E
55200	2001 RO19	14	-70	186	-58	18.3910					233	E

Table 1. continued.

number	Asteroid name/designation	λ_1 [deg]	β_1 [deg]	λ_2 [deg]	β_2 [deg]	P [h]	P_{LCDB} [h]	A_{min} [mag]	A_{max} [mag]	U	N	method
64480	2001 VG45	128	-60	265	-72	6.49717					233	E
66076	1998 RD53	100	-54	233	-66	8.93855					485	E
69117	2003 EX2	13	70			4.74608					215	E
71011	1999 XE45	91	-24	264	-31	4.69449					115	C
74155	1998 QK93	264	50			15.9680					393	E
75167	1999 VF128	190	-56	350	-55	10.27743					280	C
75495	1999 XM181	64	-32	252	-64	14.69041					200	E
76214	2000 EV64	168	28			9.27775					132	C
77677	2001 MA25	139	-69	326	-55	5.304712					253	E
78420	2002 QU40	123	-46	327	-45	4.91365	4.90		1.1	2	193	E
79436	1997 TD6	70	-53	201	-68	3.635352					207	E
80112	1999 RN61	70	-58	247	-39	4.923622					157	E
81740	2000 JA46	100	-72	310	-47	9.34151					272	E
81911	2000 NV9	136	23	334	49	6.95480					288	E
82642	2001 PX5	53	37	241	67	11.61144					178	E
85489	1997 SV2	317	-56			5.79502					81	E
85532	1997 WD21	117	-75			4.76820					230	E
89764	2002 AW61	8	-45	152	-60	5.93513					278	E
91063	1998 FX62	53	-44	191	-60	11.66510					255	C
94808	2001 XM167	9	-59	197	-63	10.66092					104	E
96461	1998 HS36	166	-60	344	-72	12.67641					115	E
97346	2000 AF10	11	42	222	50	7.65364					394	E
99667	2002 JO1	86	-57	262	-42	5.07877					199	C

Table 2. List of new asteroid models derived from a restricted period interval centered at P_{LCDB} . The meaning of columns is the same as in Table 1. Asteroids marked with * were independently confirmed by Hanuš et al. (2016).

number	Asteroid name/designation	λ_1 [deg]	β_1 [deg]	λ_2 [deg]	β_2 [deg]	P [h]	P_{LCDB} [h]	A_{min} [mag]	A_{max} [mag]	U	N	method
60	Echo	91	-25	272	-17	25.2285	25.208	0.07	0.22	3	446	E
116	Sirona	51	-53	222	-53	12.03251	12.028	0.42	0.55	3	454	C
138	Tolosa	49	-42	222	-39	10.10306	10.101	0.18	0.45	3	528	E
176	Iduna	83	24	219	68	11.28784	11.2877	0.14	0.43	3	491	E
214	Aschera	123	-37	306	-42	6.83369	6.835	0.20	0.22	3	386	E
239	Adrastea	226	-70			18.4717	18.4707	0.34	0.51	3	416	E
270	Anahita*	30	-35	205	-48	15.05950	15.06	0.25	0.34	3	492	C
353	Ruperto-Carola*	47	-55	220	-46	2.738962	2.73898		0.32	3	368	E
391	Ingeborg*	305	-52			26.4149	26.391	0.22	0.79	3	409	E
394	Arduina*	0	-79	191	-49	16.62157	16.5	0.28	0.54	3	395	CE
513	Centesima	149	4	332	15	5.32399	5.23	0.18	0.45	3	460	C
636	Erika	13	-70	176	-60	14.60771	14.603	0.29	0.33	3	498	E
670	Ottegebe*	127	77	304	68	10.03991	10.045	0.34	0.35	3	540	C
682	Hagar*	93	-71	277	-35	4.850417	4.8503	0.49	0.52	3	334	C
700	Auravictrix	54	33	249	47	6.07489	6.075	0.18	0.43	3	404	CE
706	Hirundo*	91	70	250	45	22.0161	22.027	0.39	0.9	3	365	E
744	Aguntina	44	-58	227	-51	17.4690	17.47		0.50	3	388	CE
762	Pulcova*	20	-12	196	-42	5.83977	5.839	0.18	0.30	3	408	E
769	Tatjana	176	54	347	38	35.0637	35.08	0.30	0.33	3-	437	E
844	Leontina	302	68			6.78303	6.7859	0.20	0.26	3	415	E
885	Ulrike	13	-64	207	-60	4.906164	4.90	0.55	0.72	3	416	C
918	Itha	59	-59	249	-72	3.473810	3.47393	0.15	0.30	3	350	E
943	Begonia	209	-75			15.6593	15.66	0.24	0.34	3	363	E
968	Petunia	355	-78			61.160	61.280		0.38	3	361	CE
979	Ilsewa	352	-66			42.8982	42.61	0.30	0.31	3	370	E
1077	Campanula	178	76	313	59	3.850486	3.85085	0.24	0.40	3	361	E
1083	Salvia	165	-59	358	-58	4.281429	4.23		0.61	3	277	C
1150	Achaia*	126	-65	315	-60	61.071	60.99		0.72	3	396	CE
1294	Antwerpia	128	-66	246	-76	6.62521	6.63	0.35	0.42	3	317	E
1332	Marconia	37	31	220	31	19.2264	19.16		0.30	3	408	E
1352	Wawel*	37	55	201	52	16.9542	16.97	0.35	0.44	3	356	C
1379	Lomonosowa	72	-84	265	-46	24.4846	24.488		0.63	3	359	E
1407	Lindelof	147	36			31.0941	31.151		0.34	3	397	CE
1449	Virtanen*	89	61	302	61	30.5006	30.495	0.08	0.69	3-	354	E
1486	Marilyn*	83	-57	270	-62	4.566945	4.566	0.40	0.48	3	492	C
1496	Turku	75	-75			6.47375	6.47		0.51	3-	486	CE
1521	Seinajoki	63	-18	230	-37	4.328159	4.32		0.15	3	331	C
1592	Mathieu	94	-14	269	-7	28.4821	28.46		0.50	2+	302	E
1716	Peter	52	-60	252	-52	11.51720	11.514		0.52	3	348	CE
1723	Klemola	52	-54	239	-56	6.25609	6.2545	0.16	0.33	3	484	E
1820	Lohmann*	62	67	250	58	14.04497	14.0554	0.40	0.55	3	281	E
1833	Shmakova	88	47	336	84	3.838235	3.93		0.38	3	355	E
1858	Lobachevskij	80	50	255	48	5.41208	5.413	0.30	0.48	2+	390	E
1860	Barbarossa	45	30	238	63	3.254853	3.255	0.28	0.35	3	404	E
1906	Naef	72	-70			11.00818	11.009	0.92	0.96	3	319	C
2064	Thomsen	118	-72	334	-56	4.244023	4.233		0.62	3	550	E
2275	Cuitlahuac	9	-65			6.29005	6.2891		1.10	3	536	E
3015	Candy	142	-26	346	-70	4.625223	4.625	0.50	1.05	3	450	E
3773	Smithsonian*	121	-62			6.98132	6.9804		1.04	3	622	C
4089	Galbraith	64	69	218	50	4.91316	4.9123		0.68	3	687	C
4265	Kani*	74	67	277	72	5.727574	5.7279		0.75	3	730	CE
4641	1990 QT3	178	-46	359	-50	5.313079	5.3126		0.88	3	541	C
4801	Ohre	121	-74	266	-85	31.9990	32.000	0.50	0.60	3	581	CE
4896	Tomoezozen	276	-66			8.87996	8.869		0.65	3	371	CE
4995	1984 QR	243	68	355	70	26.3920	26.37		0.82	3-	261	E
5738	Billpickering	2	-66			10.38264	10.4		0.45	3	118	E
6406	1992 MJ*	17	-61	216	-52	6.81816	6.819	1.10	1.18	3	508	CE
6487	Tonyspear	165	-90			74.501	74.91		1.24	3-	372	C
6510	Tarry	84	-72	249	-37	6.36490	6.370	0.50	0.54	3	376	E

Table 2. continued.

number	Asteroid name/designation	λ_1 [deg]	β_1 [deg]	λ_2 [deg]	β_2 [deg]	P [h]	P_{LCDB} [h]	A_{min} [mag]	A_{max} [mag]	U	N	method
7783	1994 JD	70	-71			31.8661	31.83		0.85	3	265	E
9983	Rickfienberg	120	-58	248	-77	5.29616	5.2963		1.30	3	371	C
12045	Klein	77	-22			9.00648	8.9686		0.55	3-	453	E
14257	2000 AR97	57	67			13.57929	13.584		0.67	3	514	C
28887	2000 KQ58*	11	-61	191	-21	6.84315	6.8429		0.55	3	368	E
31485	1999 CM51	94	-36	316	-56	6.00262	6.001	0.65	0.68	3	375	E
34484	2000 SR124*	236	-55			6.17519	6.174		0.80	2+	473	C
44600	1999 RU10	267	-24			6.21130	6.211	0.98	1.09	3	310	C
80276	1999 XL32	60	38	275	63	5.57148	5.56		0.77	3-	258	C
88161	2000 XK18	195	53	340	70	6.80480	6.806		0.80	3	429	C